Available online at www.sciencedirect.com
ScienceDirect
Journal of Power Sources 160 (2006) 27–36
JOURNAL OF POWER SOURCES
www.elsevier.com/locate/jpowsour

Improving the performance of high-temperature PEM fuel cells based on PBI electrolyte

F. Seland *, T. Berning [1], B. Børresen, R. Tunold

Electrochemistry Group, Department of Materials Science and Engineering, Norwegian University of Science and Technology, NO-7491 Trondheim, Norway

Received 12 January 2005; received in revised form 30 December 2005; accepted 4 January 2006
Available online 28 February 2006

Abstract

This paper describes the testing of the gas-diffusion electrodes for polymer electrolyte membrane fuel cells utilizing phosphoric acid doped polybenzimidazole (PBI) electrolyte, which allows for an operating temperature as high as 200 °C. In order to determine the optimum structure of our anodes and cathodes, the platinum content in the Pt/C catalyst and catalyst loading were varied, as well as the loading of the PBI electrolyte dispersed in the catalyst layer. The different MEAs were tested in terms of their performance by recording polarization curves using pure oxygen and hydrogen. It was found that a high platinum content and a thin catalyst layer on both anode and cathode, gave the overall best performance. This was attributed to the different catalyst surface areas, the location of the catalyst in relation to the electrolyte membrane and particularly the amount of PBI dispersed in the catalyst layer. Scanning electron microscopy (SEM) was used in order to examine the cross-section of the MEAs and measure the thickness of the catalyst layers. With this information, it was possible to give an estimate of the porosity of the catalyst layer.

Keywords: PEM; Fuel cell; Polybenzimidazole; PBI; CO poisoning; Electrocatalysis

1. Introduction

As PEM fuel cells approach commercialization there is an increased desire to raise the operating temperature to above 100 °C. To date, most PEM fuel cells are based on an electrolyte that relies on addition of liquid water to facilitate protonic conduction. Operating these fuel cells at a temperature close to the boiling point of water introduces a dual phase water system that must be controlled carefully. Common problems are the possible drying out of the electrolyte membrane at the anode at high current densities and possible flooding of the gas-diffusion electrodes due to water condensation. A lot of work has been focussed on resolving the water-management issues related to these fuel cells, e.g. [1–4].

Polymer electrolyte fuel cells based on polybenzimidazole (PBI) electrolyte represent a new generation of PEM fuel cells that can be operated at temperatures up to 200 °C. An increased operating temperature significantly increases the tolerance towards carbon monoxide, as has previously been shown by Li et al. [5] and Holladay et al. [6]. Li et al. report a CO tolerance of 3% CO in hydrogen at current densities up to 0.8 A cm^{-2} at 200 °C and 0.1% CO in hydrogen at 125 °C and current densities lower than 0.3 A cm^{-2}, where CO tolerance is defined by a voltage loss less than 10 mV. Furthermore, the electro-osmotic drag coefficient for water and methanol in phosphoric acid doped PBI membranes has been reported by Weng et al. [7] to be essentially zero under all conditions. This greatly simplifies the material balances and mass transport management and reduces the crossover of methanol in direct methanol fuel cells. High-temperature PBI fuel cells offer a viable alternative to low-temperature PEM fuel cells that demand an extensive and expensive pre-treatment of the fuel.

Polybenzimidazole, PBI, is an amorphous basic polymer with a high thermal stability and a reported glass transition temperature of 420 °C [8]. The conductivity of different PBI membranes in the pure state is very low and about 10^{-12} S cm^{-1} [9,10]. However, there are many ways of substantially increase the conductivity of PBI membranes, and this has been the focus in several recent published works, e.g. [11–16]. Polybenzimida-

* Corresponding author. Tel.: +47 73594040; fax: +47 73594083.
E-mail addresses: frode.seland@material.ntnu.no (F. Seland), torsten.berning@de.opel.com (T. Berning), borre.borresen@material.ntnu.no (B. Børresen), reidar.tunold@material.ntnu.no (R. Tunold).
[1] Present address: Adam Opel AG, International Technical Development Center, D-65423 Rüsselsheim, Germany.

0378-7753/$ – see front matter © 2006 Elsevier B.V. All rights reserved.
doi:10.1016/j.jpowsour.2006.01.047

zole reacts easily with acids, and phosphoric acid is the most frequently used dopant. Phosphoric acid undergoes hydrogen bond interaction or proton transfer reactions with basic polymers, and shows remarkable high proton conductivity even in anhydrous form, due to its unique proton conduction mechanism [17–19]. The idea to use PBI membranes doped with phosphoric acid as an electrolyte in fuel cells was first introduced by Wainright et al. [20]. The proton conductivity of phosphoric acid doped PBI is influenced by relative humidity, temperature and acid doping level as reported by Ma et al. [15]. Conductivity increases with increasing temperature following an Arrhenius equation. At high doping levels of phosphoric acid (i.e. 630%) they reported that conductivity increases significantly with relative humidity mainly due to the interaction of water with excess acid. Li et al. [21] reported the presence of strong hydrogen bonds between phosphoric acid and nitrogen atoms of the imidazole rings by infrared and Raman spectroscopy. They found that only two molecules of phosphoric acid are bonded to each repeat unit of PBI. An excessive doping of acid is "free acid" and contributes to the high conductivity. The upper limit of proton transfer is thus given by the conductivity of the H_3PO_4 in liquid state. In a work done by He et al. [14] the conductivity of PBI was found to be as high as 6.8×10^{-2} S cm^{-1} at 200 °C with a H_3PO_4 doping level of 560% and 5% relative humidity.

The development of a high proton-conducting PBI membrane, due to the extensive study by several groups, has notably decreased the voltage loss over the membrane and brought forward the necessity of switching the attention from the membrane to other aspects of the fuel cell. Further research and development of i.e. electrocatalysis and bipolar plates, are important in order to further improve the fuel cell performance. It was found by Barbir et al. [22] that the contact losses that occur at the interface between the bipolar plates and the backside of the gas-diffusion electrodes can be as high as 0.150 Ω cm^2. This value corresponds to the resistance through an 80 μm membrane with a conductivity of 5.33×10^{-2} S cm^{-1}, and demonstrates the need of improving the bipolar plates in both materials and channel geometries.

The focus in our work has been to understand the importance of a carbon support layer, improve single cell performance by varying the composition of the catalyst layer, and manufacturing of single membrane electrode assemblies by hot-pressing. Instead of describing the multitude of different MEAs manufactured, this paper will focus on the outcome of our study, highlighting the main observations. This is best done by describing the function of each of the electrode layers. It has been found in several studies of PEM fuel cells that the type and composition of the catalyst is crucial for the cell performance. The electrodes were manufactured at our department with use of commercial catalyst (platinum on carbon) with various platinum contents. The catalyst loading as well as the PBI loading inside the catalytic layer were varied.

2. Experimental

The electrodes described in this paper were prepared by manual spraying with an airbrush (Badger No. 100G). This method allowed for the accurate determination of the catalyst loadings as well as for a good reproducibility, and minimized loss of catalyst in the spraying procedure. Carbon fibre paper was purchased from Toray (TGP-H-120) while the carbon black (Vulcan XC-72) used in the carbon support layer was provided by Cabot Corporation. The electrocatalysts, HiSPEC^{TM} 3000 (20% Pt on Vulcan XC-72R), HiSPEC^{TM} 4000 (40% Pt on Vulcan XC-72R) and HiSPEC^{TM} 8000 (50% Pt on Vulcan XC-72R), were purchased from Johnson & Matthey. PBI membranes were provided by the Department of Chemistry, Technical University of Denmark (DTU), as a partner in the European 5th Framework Programme, contract no. ENK5-CT-2000-00323, which is acknowledged.

2.1. MEA preparation

Due to the poor mechanical strength of the catalyst layers, they are deposited on a rigid backing or substrate. In this work, carbon fibre paper (Toray; TGP-H-120) was wet-proofed by immersing it in a 20% polytetrafluorethylene, PTFE-solution (DU PONT) and hot-baked at 360 °C for 30 min in order to polymerize the PTFE. The weight increase for the wet-proofed paper compared with the non-wet-proofed paper was in the order of 20%. The PTFE was found to accumulate predominantly at the fibre crossings, thus reducing the porosity of the carbon fibre paper. The benefit of wet-proofing in this case lies in the prevention of the paper from soaking during the spraying procedure and reduces the penetration of carbon particles into the paper. This actually leads to a higher total porosity for the complete electrode by wet-proofing the carbon paper, most likely due to a lower pore size. Since wet-proofing normally helps in terms of water management, the effect of PTFE on the cell performance in itself at an operating temperature of 175 °C was found to be insignificant. However, when spraying the carbon support layer onto the carbon fibre paper, it was found that the bonding between the carbon support layer and the fibre paper was improved by wet-proofing.

2.1.1. Carbon support layer

Although the carbon fibre paper provides a fairly smooth substrate on which the catalyst layer may be directly deposited, the need of a carbon support layer was found to be of much higher importance than first believed. Reproducible results were first obtained after extensively testing of the different preparation steps. The carbon support layer has several functions: (i) to prevent the catalyst from penetrating into the carbon fibre paper, (ii) to ensure a good electronic bonding between the carbon fibres and the catalyst layer, (iii) to provide a pathway for the supply of reactants and the removal of product water and (iv) to obtain a smooth and uniform surface on which the catalyst is deposited.

Depending on the spraying conditions (solvent, air flow, nozzle size and temperature) three distinct structures of the carbon support layer can be made, as shown in Fig. 1. Fig. 1a shows the first structure which possesses a similar texture as the underlying carbon fibre structure, with the carbon powder evenly distributed on top of each fibre. It was a result of spraying with a solvent that rapidly evaporates (e.g. isopropanol). Secondly, Fig. 1b,

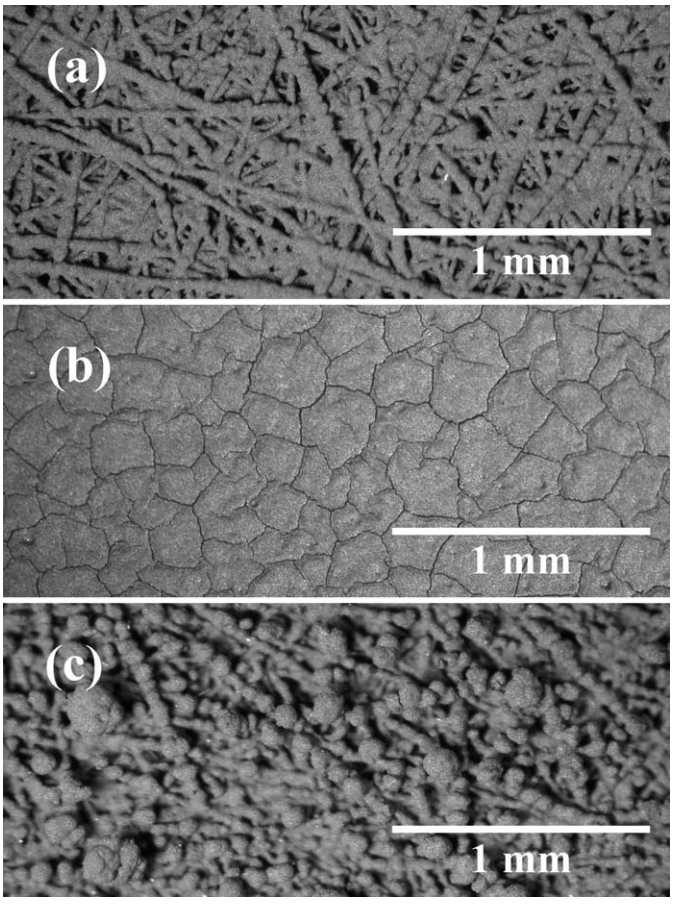

Fig. 1. Light microscope pictures of the three distinct surface structures that the support layer obtained in this work: (a) fibre structure, (b) mud crack structure and (c) dendrite structure.

demonstrates a mud cracked structure with large islands and thin crevices that provided a smooth and flat surface. This structure was a result of using water as the solvent. Finally, Fig. 1c, shows a carbon dendrite structure with many carbon spikes, and was typically achieved when the nozzle was clogging or a too high air flow was applied during spraying.

To obtain good adhesion of the carbon particles to the fibres in the underlying carbon paper, structure 1 (Fig. 1a) was found beneficial and offered a good electronic contact as well. Therefore, after making structure 1 on top of the carbon backing we made the mud crack structure (Fig. 1b) on top of this. A total amount of 2 mg cm^{-2} carbon black was found to be sufficient to produce the desired support layer.

2.1.2. Catalyst layer

The catalyst layer is a key element in a fuel cell. It is important that the platinum catalyst is in close contact with the polymer membrane (electrolyte), the reaction gases and the current collector, and at the same time facilitates the transport of depleted reactants and product water out of the catalyst structure without impeding the supply of fresh reactants.

In order to obtain a catalyst layer with PBI dispersed in the layer, PBI was dissolved in concentrated dimethylacetamide (DMAC), and catalyst particles were dispersed in this solution.

Table 1
Anodes created for this study

Electrode name	Pt loading (mg cm^{-2})	Catalyst type (% Pt/C)	PBI loading (mg cm^{-2})
Anode 1, A1	0.30	20	0.30
Anode 2, A2	0.40	20	0.40
Anode 3, A3	0.40	20	0.60
Anode 4, A4	0.40	50	0.24
Anode 5, A5	0.40	50	0.36
Anode 6, A6	0.40	50	0.48

Table 2
Cathodes created for this study

Electrode name	Pt loading (mg cm^{-2})	Catalyst type (% Pt/C)	PBI loading (mg cm^{-2})
Cathode 1, C1	0.50	20	0.50
Cathode 2, C2	0.60	20	0.60
Cathode 3, C3	0.60	40	0.36
Cathode 4, C4	0.60	50	0.36
Cathode 5, C5	0.60	50	0.60

This dispersion was then sprayed slowly onto the support layer described above. In this work the catalyst type and loading as well as the PBI loading inside the catalyst layer was varied. Table 1 lists the anodes that were used in this study and Table 2 lists the cathodes used. Cathode C1 was used as the reference cathode when studying the anodes, while anode A2 was used as the reference anode to the different cathodes.

At the cathode side mass transport limitations probably become more significant than at the anode side. As a result, the local current generation inside the cathodic catalyst layer would shift away from the electrolyte membrane, which leads to a higher IR loss in this layer. Clearly, there must be an optimum catalyst distribution both on the anode and cathode side, as well as an optimum with respect to the amount of PBI in the mixture. Careful studies have been undertaken in order to find the optimum amount.

From earlier experiments performed at our department, a loading of equal amounts (weight) of platinum and PBI was considered standard. Note, however, that the PBI loading should, in theory, be scaled to the expected surface area of the catalyst, not to the overall amount. A scaling with the specific volume of the catalyst powder should yield similar results.

The reason why the anode side may be critical for this type of fuel cells is that the thickness of the catalyst layer may play an important role. On the other hand, the mass transport limitations for hydrogen are much lower than for oxygen due to the higher diffusivity of hydrogen. This implies that the local current density on the anode remains close to the electrolyte membrane, as long as sufficient catalyst area is provided. As a result, the 50% Pt/C, which provides the highest surface area per unit volume, should intuitively be the catalyst of choice at the anode side.

It should be mentioned that even with the spraying technique it is not possible to obtain exactly the desired loadings, but an effort was made to keep the final amount of platinum within 5% of the desired quantity.

2.1.3. Acid doping, hot-pressing and testing of MEAs

After spraying the catalyst layer consisting of catalyst and PBI in DMAC, the electrodes were heated for 3 h at 180 °C in order to evaporate the remaining solvent. Li et al. report that a drying temperature of up to 190 °C for hours is necessary to remove traces of DMAC [23]. The final step of preparing the electrodes is to dope the PBI in the catalyst layer with phosphoric acid by spraying. In this work we used a constant weight ratio of 6:1 between the phosphoric acid and the PBI. It is believed that the percentage of the acid will be evened out by diffusion with time, and besides, the membrane contains much more acid so that the acid loading is assumed to be less critical.

The membrane electrode assemblies (MEAs) were made by hot-pressing a sandwich of 2 cm × 2 cm electrodes and a 4 cm × 4 cm PBI membrane (which were previously doped in 75 wt.% phosphoric acid) at 130 °C for 25 min with a pressure of 25 kg cm^{-2}. The MEAs were tested in a commercially available single cell fuel cell with one reference electrode probe and 5 cm^2 double serpentine flow field (ElectroChem, Inc.), originally designed for low-temperature PEM fuel cells. In order to ensure that the PBI in the catalyst layer and the membrane was completely saturated with phosphoric acid, the MEAs were cured for 2 weeks at ambient temperature after the hot-pressing and then tested.

The polarization curves of all our membrane electrode assemblies were recorded at different temperatures, but with focus on 175 °C as a default temperature. The fuel cells were tested with pure hydrogen and oxygen (instrumental grade 2.0) and a sufficient pressure was applied to cause a flowrate of 1.47 cm^3 s^{-1} oxygen and 3.60 cm^3 s^{-1} hydrogen.

2.2. Theoretical considerations

In this study, the effect of different platinum catalyst types (platinum on carbon, Pt/C) and composition on the fuel cell performance was investigated. The Pt/C catalysts were provided by Johnson & Matthey, and relevant information is listed in Table 3. In heterogeneous catalysis the available active surface area is of major importance, and hence the 20% Pt/C powder seems to offer the best value as the total metal area per gram is by far the largest. This is also demonstrated by the higher roughness factor that this catalyst may obtain. It is worth noticing that there is no obvious relation between mass activity and particle size of the catalyst. Kinoshita showed that the specific activity of the reduction of oxygen on supported Pt particles in acid electrolytes increases with an increase in particle size [24].

The overall thickness of the catalyst layer, when using 20% Pt/C, is at least twice the thickness when either 40% or 50% Pt/C is being used. It was shown by for example Bevers et al. [28] in their work with Nafion® fuel cells, that most of the catalytic activity takes place in areas close to the electrolyte membrane, typically within the first 10 μm. This might be different for PBI fuel cells, because in terms of the permeability to the reactants the PBI exhibits different values, which should affect the current distribution inside the catalyst layer. Due to elevated temperatures, reaction kinetics is also of importance.

Table 3
Summary of catalyst and catalyst layer

Catalyst type (nominal) and electrode name	20% Pt/C (C2)	40% Pt/C (C3)	50% Pt/C (C4)
Catalyst measured[a] (wt.% Pt)	19.96	39.67	48.65
Average Pt particle size[a] (nm)	2.6	3.54	3.51
Minimum metal surface area[a] ($m^2_{Pt}\,g^{-1}_{Pt}$)	90	60	50
Theoretical roughness[b] ($m^2_{Pt}\,m^{-2}_{geo}$)	540	360	300
Theoretical specific Pt area[c] ($m^2\,cm^{-3}$)	13	23	27
Theoretical thickness of catalyst layer[c] (μm)	15.3	6.9	5.6
Real catalyst layer thickness[d] (μm)	47	14	7
Estimated porosity[c] (%)	67	51	20

[a] Data as provided by Johnson Matthey Corp.
[b] Assumes that the entire Pt surface area is active and a loading of 0.6 mg cm^{-2}.
[c] Based on a loading of 0.6 mg Pt cm^{-2} and assuming a density of 2270 kg m^{-3} of the carbon [25], 21,440 kg m^{-3} for the platinum [26] and 1350 kg m^{-3} as the ultimate density for PBI [27].
[d] Real catalyst layer thickness as determined from SEM scans.

A theoretical thickness of about 40 μm can roughly be estimated for a cathode using 20% Pt/C catalyst with a Pt loading of 0.5 mg, 0.5 mg cm^{-2} PBI and with a porosity of 65–70%. This value is in the range of the membrane thickness, and this could perhaps lead to lower performance due to limited protonic migration inside the catalyst region especially at elevated current densities and if the electronic percolation present in the layer is not sufficient.

At low current densities, only a small fraction of the available catalyst area is needed, and the current will be generated at the energetically favoured sites. These sites are likely to exist near the electrolyte membrane since it is easier for the reactant gases to diffuse through than for the protons to migrate through the catalyst layer. However, with increased current density, the reactant gases become more and more depleted, and the local current generation shifts away from the membrane interface. This may also be caused by the fact that the energetically favoured sites are occupied. This means that the protons have to migrate further. Because of the fact that the catalyst layer consists only of a small fraction of PBI electrolyte, the losses associated with the protonic migration can be of the same magnitude or even higher than the ohmic losses in the membrane. Thus, it is important to provide a high catalyst area in a region close to the membrane interface without starving the cell of reactants, which occurs when too much electrolyte is needed. This is of particular importance at the cathode side of the PBI fuel cell, because the permeability for oxygen through phosphoric acid doped PBI at 150 °C is much lower than through Nafion®-117 at 80 °C, 10^{-9} and 9×10^{-9} cm^3 (STP) cm cm^{-2} s cmHg, respectively [29,30].

3. Results and discussion

3.1. Open circuit voltage

The open circuit voltage (OCV) is the maximum voltage that can be achieved in a fuel cell with zero loading. Normally, the

Table 4
Open circuit voltages for selected cells at 125 and 175 °C

MEA	A2C1	A2C2	A2C3	A2C4	A2C5	$A5C5_{ii}$
E_{OCV} (mV), 125 °C	870	850	855	845	860	770
E_{OCV} (mV), 175 °C	880	880	900	890	885	805

value of the OCV lies close to the thermodynamic equilibrium potential i.e. as is observed in a hydrogen/chlorine fuel cell [31]. In other cases it can be considered as a mixed potential. In this study, the open circuit voltage varied from one MEA to another, but usually in the range 840–900 mV depending on the operating temperature and MEA characteristics. The open circuit voltages are given in Table 4.

In a H_2/O_2 fuel cell, the measurement of the thermodynamic rest potential on the oxygen reduction is very difficult due to the very low exchange current density of the oxygen electrode on platinum (around 10^{-10} A cm^{-2}) [32]. As a consequence to this, the measurement of the open circuit potential is easily influenced by any side reactions, i.e. corrosion of platinum. In fact, the rest potential measured rarely exceeds 1.1 V versus the NHE even on a very active platinum electrode in purified acid or alkaline aqueous solution, with 1 atm of oxygen and ambient temperature [33]. The most frequently reported open circuit potentials for oxygen electrodes in Nafion®-based fuel cells are around 1.0 V versus the NHE.

Extensive research has been done in order to minimize the polarization losses on the cathode by improving the kinetics of the oxygen reduction reaction. A part of the problem is that the complete reduction of oxygen to water involves four successive electron transfer steps that are particularly slow in phosphoric acid environment due to the presence of the bulky phosphate anions adsorbed at the catalyst surface.

The anode operates at a potential just above the reference hydrogen potential and under such highly reducing conditions that carbon has low probability to corrode. On the other hand, when the fuel cell is operated at low current densities, the potential at the cathode can be about 0.7 V above that of the anode and even higher at open circuit. Carbon will oxidize to carbon dioxide at this potential, but only at a very slow rate [34]:

$$C + 2H_2O \rightarrow CO_2 + 4H^+ + 4e^- \quad (1)$$

Such anodic back reactions are another reason why fuel cells with carbon supported catalysts do not give the thermodynamic equilibrium voltage for the hydrogen/oxygen reaction at open circuit.

In this work an increase, usually around 30 mV, in the open circuit voltage was observed, as the temperature was increased from 125 to 175 °C. This is believed to be due to better kinetics as the temperature increases and that the exhaust water in gaseous state will leave with less hindrance at a higher temperature.

The most likely reason for the low open circuit voltage, however, is fuel cross-over, i.e. hydrogen cross-over in a H_2/O_2 fuel cell, that establishes a mixed potential on the cathode. Using a thin membrane the resistance to cross-over of reaction gases through the membrane is lower and a more pronounced effect of a mixed potential is expected. Thus the electrode potential and the corresponding open circuit voltage of the fuel cell will decrease. This was observed by the low open circuit voltage obtained by using a thin membrane (25 μm) in the MEA denoted $A5C5_{ii}$ compared to the open circuit values for the other MEAs (thickness around 40 μm). One of the most critical issues when operating a fuel cell is the chance of puncturing the membrane and thus creating an easy path for reaction gases to the opposite electrode. This is the most likely reason why an MEA stops functioning and thus leads to an extremely low open circuit voltage. Puncturing or cracking of the membranes is particularly critical when operating a fuel cell stack.

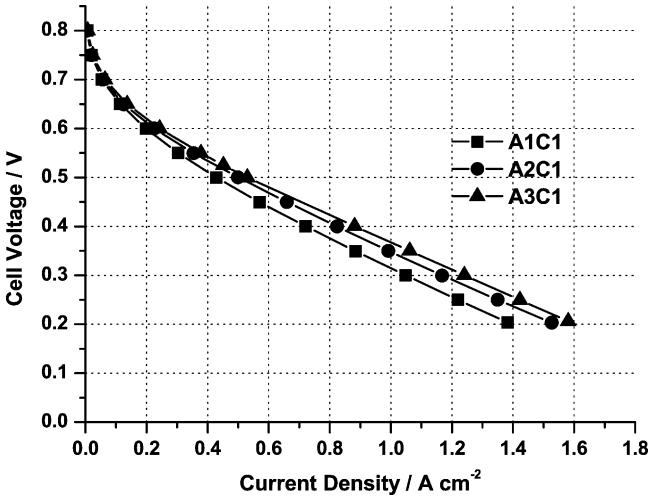

Fig. 2. Polarization curves for A1C1 (squares), A2C1 (circles) and A3C1 (triangles) at 175 °C.

3.2. Anode side

Fig. 2 shows the polarization curves at 175 °C for MEAs where the loading of the platinum catalyst and the amount of PBI in the catalyst layer of the anode is varied. See Table 1 for relevant information. Note again that the electrode composition used at the cathode side was the same in all cases and equal to cathode C1 (Table 2). Inconsistencies in the spraying technique, hot-pressing, membrane thickness or cutting of 2 cm × 2 cm electrodes could lead to small changes in performance. However, after continuously improving our testing procedure, we found the performance of the MEAs to be quite reproducible.

As seen from Fig. 2, the effect of an increase in catalyst loading on the anode side was found to be relatively strong, as opposed to Nafion® fuel cells, where the effect of the anode side is usually neglected. This is apparently not the case with PBI fuel cells, where the hydrogen oxidation may be more lethargic in the phosphoric acid environment. Fig. 2 shows the polarization curves of A1C1, A2C1 and A3C1, and an improvement of current density was found to be around 15–20% at a cell voltage of 500 mV when increasing the platinum loading from 0.3 to 0.4 mg cm^{-2}. A further increase in the current density of somewhat less than 10% was previously found when the loading was increased to 0.6 mg cm^{-2} on the anode side. The effect

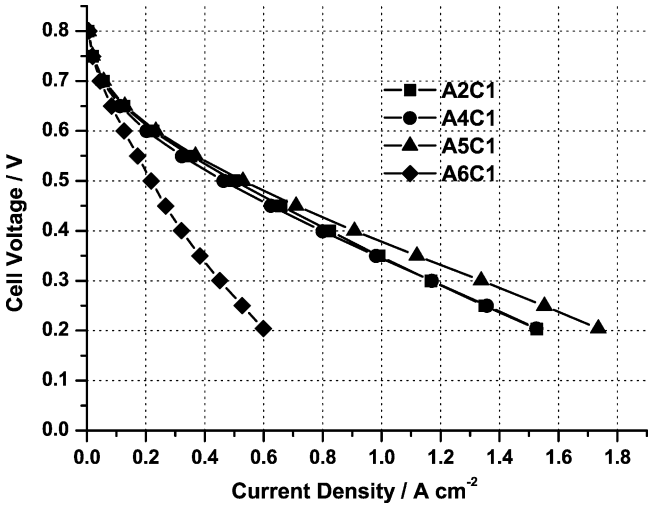

Fig. 3. Polarization curves for A2C1 (squares), A4C1 (circles), A5C1 (triangles) and A6C1 (diamonds) at 175 °C.

of catalyst loading was found to be even more pronounced at 125 °C.

Based on this finding we conclude that the hydrogen solubility is low and the hydrogen permeability and kinetics are slow in phosphoric acid doped PBI environment compared to Nafion®, and thus an increased three-phase region (reactant, membrane and catalyst) is desired. An increased reaction zone can be achieved by increasing the platinum and PBI loading up to a certain extent, increasing the platinum content or increasing the catalyst layer thickness. However, an increased platinum content would decrease the catalyst layer thickness when equal amount of platinum is to be used, so there will be a compromise between the two.

By comparing the performance of the cells A2C1 and A3C1 in Fig. 2, and A4C1, A5C1 and A6C1 in Fig. 3, an effect of increasing the PBI loading in the catalyst layer can be observed. When the PBI loading was increased by 50%, with the same type and same amount of catalyst, there was a noticeable increase in fuel cell performance implying that an increase of the amount of PBI had a beneficial effect on the performance. An increase in the PBI loading obviously enhances the protonic transport inside the catalyst layer and makes the catalyst to be used more effectively. Interestingly, the performance of A6C1 in Fig. 3 clearly demonstrates the effect of having too much PBI in the catalyst layer. The performance drops drastically and was related to the isolating and blocking of active catalyst particles by the excessive amount of PBI, thus reducing the overall oxidation rate of hydrogen.

The effect of using a higher platinum concentration on the anode side near the membrane interface could be interpreted by comparing the performance of A2C1 versus A4C1 in Fig. 3. Anode A2 and anode A4 are theoretically comparable in the platinum loading and the PBI loading, which was scaled with respect to the catalyst volume. The performance of these cells was found to be similar, although the surface area of the catalyst must be higher for anode A2. Note again that an effort was made to scale the PBI loading with the volume of Pt/C catalyst powder.

Considering the fact that anode A5 was slightly better than anode A3, and taking into account that the price of the 50% Pt/C catalyst is lower based on the amount of platinum, we conclude that using a high platinum content and relative high PBI loading in the catalyst layer yields the best performance and hence decreases the cost in making our MEAs.

3.3. Cathode side

Similar to the anode side, the various cathodes made for this study were tested, using the anode A2 given in row 2 in Table 1 for counter electrode. The cathodes prepared varied in the Pt/C catalyst composition and loading, as well as the PBI loading. Polarization curves of the corresponding fuel cells were recorded at different temperatures with 175 °C as the reference temperature. The performances of the different MEAs tested at 175 °C are given in Fig. 4.

The effect of simply increasing the amount of catalyst was observed by noticing the change in performance between A2C1 and A2C2 in Fig. 4, where the catalyst loading on the cathode side was changed from 0.5 to 0.6 mg cm^{-2}, respectively. Considering that the increase in catalyst loading is 20%, the effect on the performance is low, resulting in an increased performance of around 5%. It was found that when increasing the temperature, the performances of cathodes C2, C3 and C4 became almost identical. However, cathode C5 clearly showed an advantage over the other cathodes at 175 °C. The performance was superior in all potential regions. Of all the cathodes tested in Fig. 4, cathode C5 had the highest PBI loading based on catalyst volume, and we can conclude that a high amount of PBI was advantageous on the cathode side.

The differences between the different cathodes, except cathode C5, were relatively small compared to the differences that occurred when using different anodes. This was an interesting and unexpected finding, which indicates that a lot of the losses in this type of fuel cells are related to the limited permeability of

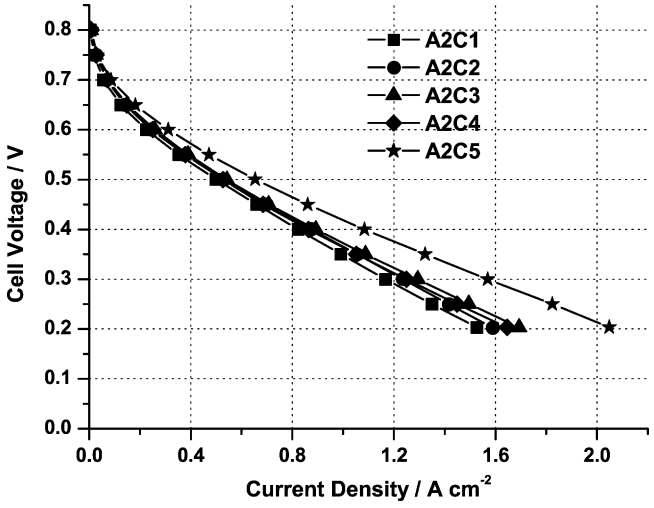

Fig. 4. Polarization curves of five MEAs with varying cathodes at 175 °C, A2C1 (squares), A2C2 (circles), A2C3 (triangles), A2C4 (diamonds) and A2C5 (stars).

the reactant gases at the catalyst layers and solubility of reactants in the dispersed PBI particles.

3.4. Platinum and PBI loading inside the catalyst layer

The catalyst layer is important in many ways and critical when it comes to cell design. It has to be ensured that on one side the reactants (e.g. oxygen) have access to the platinum surface, but on the other side the protons, which are being conducted through the electrolyte, must be able to reach the reaction site. As a consequence, it is desirable to have a thin film of electrolyte material covering the catalyst to facilitate the transport of protons. Because of the numerous transport phenomena that occur inside the catalyst layer, the exact amount of PBI has to be carefully determined for optimum cell performance.

An important finding here was that it takes a few days for the PBI to absorb the phosphoric acid and hence become a good protonic conductor. This means that during the first days the performance of the cell changes considerably, which complicated the testing procedures. As a remedy for this we decided to let all our MEAs cure for 2 weeks at ambient temperature before testing them. This ensured that the PBI was satisfactorily doped with phosphoric acid and provided reproducible results.

In this study we have found that the amount of PBI is one of the most important parameters in order to improve the fuel cell performance. The function of the PBI inside the catalyst layer is obviously to provide a path for the protons to reach the platinum surface, where the reaction occurs. The oxygen and hydrogen have to dissolve into the PBI and diffuse towards the platinum. This means that the PBI has to be a protonic conductor, and at the same time have a high solubility and diffusivity for the reactants. A high amount of PBI will improve the protonic transport on one hand, but also it will make it more difficult for the reactants to reach the platinum surface, hence it will cut off the current significantly as clearly illustrated by the performance of anode A6 in Fig. 3. A low amount of PBI means that the reactant gases can easier reach the platinum surface, but at the same time it limits the proton migration inside the catalyst layer. It is important that the solubility of oxygen and hydrogen in PBI is high, and work concerning ways of increasing solubility should be of high priority.

It appears logical that the amount of PBI mixed into the catalyst layer should be scaled with the expected surface area of the platinum rather than with the weighed amount of platinum. The amount of PBI was tested in a parametric study and the amount of PBI used in anode A5 and cathode C5, 0.36 and 0.6 mg cm^{-2}, respectively, was found to be the optimum among the electrodes tested in this study. In fact, the polarization curves obtained with the various electrodes indicate that A5 and C5 are the best anode and cathode compositions, respectively. The overall platinum loading is 1.0 mg cm^{-2} and both electrodes employed the 50% Pt/C catalyst. The resulting cell performance and power density curves when the best anode and the best cathode were combined are given for 125, 150 and 175 °C in Fig. 5. The effect of increasing the temperature is clearly seen. This is mostly due to enhanced reaction kinetics and lower IR losses.

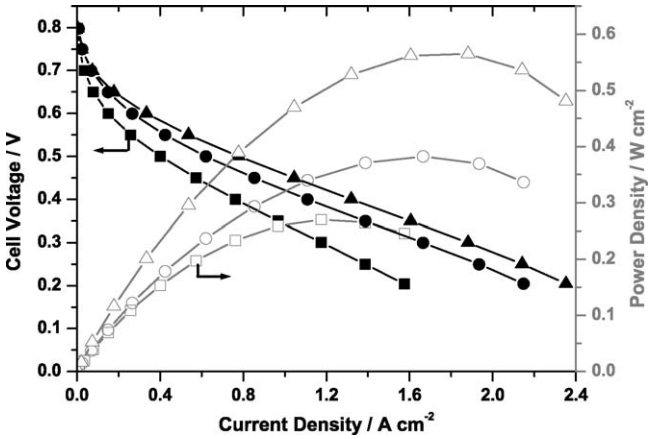

Fig. 5. Polarization curves (closed symbols) and power density curves (open symbols) at 125 °C (squares), 150 °C (circles) and 175 °C (triangles) for the MEA $A5C5_{ii}$.

3.5. Scanning electron microscopy (SEM)

Several SEM scans were performed in this study. Both surface scans of the various electrodes and cross-sectional scans of the MEAs were conducted. Backscatter mode was preferred as the catalyst layer can easily be seen since platinum shines up due to its high atomic weight. Cross-sections of the MEAs were examined by SEM after testing them. In order to obtain high quality SEM images of the cross-section near the membrane, the MEAs were broken immediately after dipping in liquid nitrogen. SEM scans also show the quality and reproducibility of the spraying technique, which in our case is satisfactorily.

Fig. 6 shows SEM pictures in backscattered mode of the MEAs A2C1, A2C2, A2C3 and A2C4, which were all used in this work. The catalyst layer can be seen as narrow bright bands on both sides of the membrane. The carbon support layer can also easily be identified as the dark region on the outside of the catalyst layer. It is easy to see how marked the difference in catalyst layer thickness appears to be between the different catalyst compositions. SEM images of the cross-section of the respective MEA provides rough estimates of the real thickness of the catalyst layer. The 20% Pt/C catalyst with a platinum loading of 0.6 mg cm^{-2} clearly gives a huge thickness of about 50 μm on the cathode side. As the cathode catalyst composition varies from 20% Pt/C (C1, C2) to 40% Pt/C (C3) and up to 50% Pt/C (C4, C5) the thickness is substantially decreased. The overall thickness of the catalyst layer (cathode side) was measured from the SEM images in Fig. 6 to be 47 μm for cathode C2 (20% Pt/C), 14 μm for cathode C3 (40% Pt/C), and as low as 7 μm for cathode C4 (50% Pt/C). The corresponding porosity of the catalyst layer was estimated to be 67%, 51% and 20% respectively (see also Table 3). This shows an even stronger dependency on platinum content than indicated by theoretical considerations. This huge difference between the expected and actually measured thickness may be due to the different properties the catalyst particles obtain in the DMAC solution due to different catalyst compositions and particle size.

It is important to note that the mud cracked morphology that is obtained after spraying the support layer (Fig. 1b) may not be

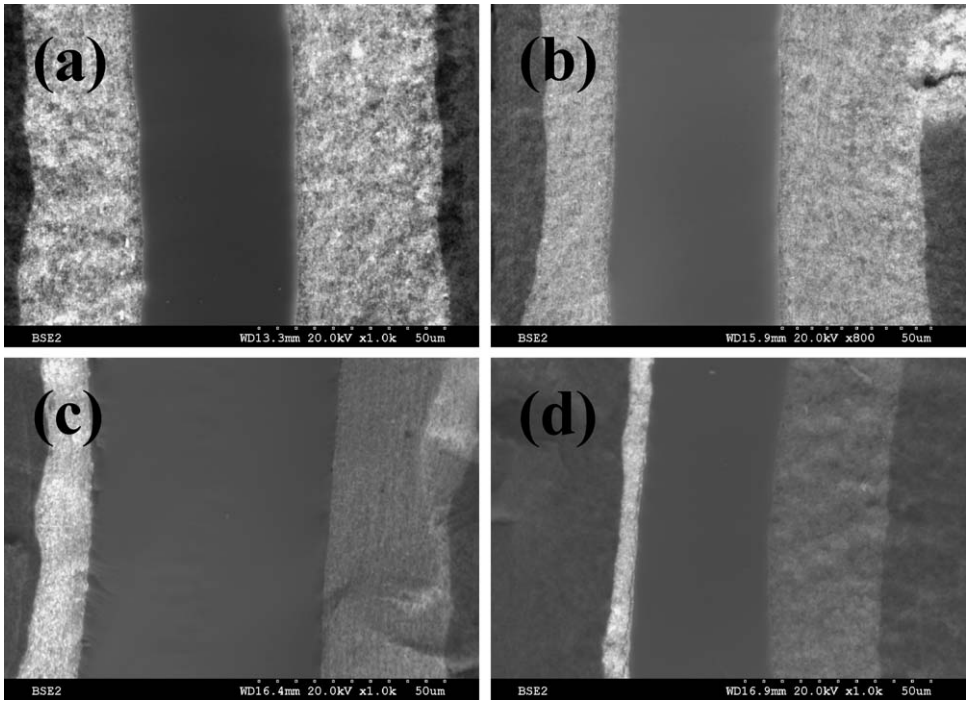

Fig. 6. Scanning electron microscopy (SEM) scans in backscattered mode of the cross-sections of the MEAs (a) A2C1, (b) A2C2, (c) A2C3 and (d) A2C4. The cathode is situated to the right side of the PBI membrane in (a) and (b), while it is situated to the left side of the PBI membrane in images (c) and (d).

the most optimal one. Due to this mud cracked structure a substantial amount of catalyst is being forced into the crevices when spraying the catalyst layer and this catalyst will not contribute to the cell performance. Fig. 7a shows a top-view SEM scan of the complete electrode, cathode C5, used in this study. A SEM picture of the cross-section of the corresponding MEA, A2C5, is given in Fig. 7b. The last picture focuses on the small crevice on the cathode side, and we can clearly see that the catalyst has been sprayed into this crevice. This is a major disadvantage of spraying catalyst onto a carbon fibre paper instead of directly onto the polymer membrane. Direct spraying onto the membrane is currently being investigated in our laboratories. When preparing electrodes separate from the membrane we conclude from this that the desired surface consists of very large islands with as small crevices as possible to limit the loss of active catalyst, but not constraining the diffusion of reactants to the reaction sites. Our electrodes have a measured crack width of about 5–10 μm (Fig. 7).

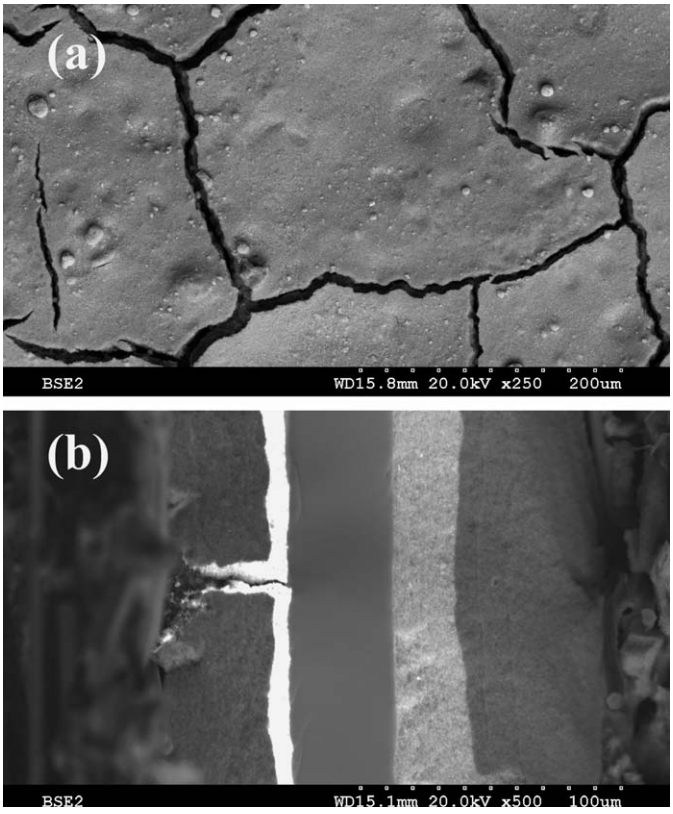

Fig. 7. SEM scans in backscattered mode: (a) top-view of cathode C5 showing the mud crack surface structure; (b) cross-section of the corresponding MEA, A2C5, with focus on the small crevice on the cathode (left) side.

3.6. Effect of membrane thickness

The thickness of the PBI membrane is varying from one research group to the other, but generally it is quite low. Case Western Reserve University group [20,35,36] and the group at the Danish Technical University (DTU) [37] make membranes about 80 μm thick. Savadogo and Xing used commercially bought (Hoechst Celanese) PBI films of 40 μm thickness [38] and obtained very nice performance of their fuel cells. Staiti et al. measured the thickness of their dried PBI membranes to be in the range of 47 ± 3 μm [39]. The PBI membranes used in this

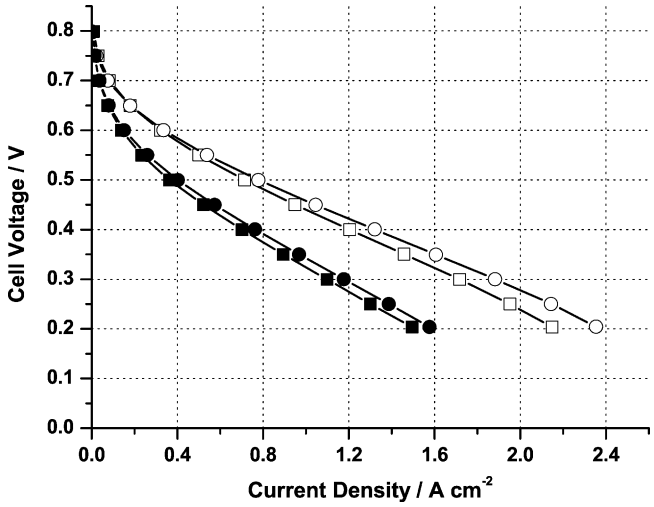

Fig. 8. Performance of two MEAs with different membrane thickness, $A5C5_i$ (40 μm, squares) and $A5C5_{ii}$ (25 μm, circles) at 125 °C (closed symbols) and 175 °C (open symbols).

work were provided by DTU with a measured thickness after hot-pressing around 40 μm.

The best anodes and cathodes in this study were put together to make MEAs denoted $A5C5_n$, where n indicates a specific MEA. We wanted to test the influence of different membrane thickness at two distinct temperatures. $A5C5_i$ is around 40 μm thick while $A5C5_{ii}$ is the thinnest one with membrane thickness of only 25 μm.

From Fig. 8 we can see that the membrane thickness is affecting the performance of the fuel cell. A thin membrane clearly enhances the performance at lower potentials while a thick membrane would supposedly show better results at higher potentials where the current density is low.

One of our largest concerns when testing our MEAs is the high possibility of puncturing the membrane while running. A thin membrane can easily break at the edges of the membrane electrode sandwich due to the stress that occurs when fitting it in our fuel cell hardware and when applying gases on both sides. Taking this into consideration, a slightly thicker membrane would make continuous testing possible and was therefore preferred ($A5C5_i$).

4. Conclusions and future work

This paper focuses on the understanding of the gas-diffusion electrodes in PBI fuel cells and their effect on the performance. Various electrodes were prepared using a spraying technique. The best performance was obtained using a catalyst of 50% Pt/C and a relative high PBI loading in the catalyst layer on both anode and cathode, anode A5 (0.4 mg cm^{-2} Pt, 0.36 mg cm^{-2} PBI) and cathode C5 (0.6 mg cm^{-2} Pt, 0.6 mg cm^{-2} PBI) respectively. The structure of the support layer was found to be of more importance than first believed. A mixture of dry and wet spraying gave the best characteristics with a good bonding to the carbon fibre paper and a good support for the catalyst layer. In order to further reduce the catalyst loading, different techniques have been proposed, such as sputtering of fine catalyst particles on top of the electrode and spraying of catalyst directly onto the polymer membrane. This will be investigated further at our department.

In addition, it was mentioned that the current tests were all performed using bipolar plates designed for low-temperature Nafion® fuel cells. These fuel cells exhibit a comparatively high amount of mass transport problems, which are in part caused by the existence of liquid water inside the gas-diffusion layers (e.g.), and partly due to the low diffusivity of the reactants, which are temperature-dependent. These phenomena have caused fuel cell manufacturers to use bipolar plates with long, serpentine channels, where a high pressure drop forces the liquid water out of the channels, or else use interdigitated designs, where a pressure drop is induced between flow channels in order to eliminate mass transport losses. The disadvantage of serpentine channels is clearly the expected uneven current distribution, as the gases will be very rich at the inlet and depleted towards the outlet. In the case of PBI fuel cells operating up to 200 °C, the mass transport problems should be significantly reduced. This should allow for the use of different bipolar plate designs with a larger shoulder width in order to reduce the contact resistance, and possibly with a higher number of parallel channels, which would result in a more even distribution of the local current densities, provided proper manifolding can be obtained.

Acknowledgments

The authors thank Dr. Gaute Svenningsen for invaluable help in preparing and performing the SEM scans. This work was funded by the European Commission in the 5th Framework Programme (Contract no. ENK5-CT-2000-00323).

References

[1] D.P. Wilkinson, H.H. Voss, K. Prater, J. Power Sources 49 (1994) 117.
[2] R. Mosdale, S. Srinivasan, Electrochim. Acta 40 (1995) 413.
[3] H.P.L.H. van Bussel, F.G.H. Koene, R.K.A.M. Mallant, J. Power Sources 71 (1998) 218.
[4] T. van Nguyen, M.W. Knobbe, J. Power Sources 114 (2003) 70.
[5] Q. Li, R. He, J.-A. Gao, J.O. Jensen, N.J. Bjerrum, J. Electrochem. Soc. 150 (2003) A1599.
[6] J.D. Holladay, J.S. Wainright, E.O. Jones, S.R. Gano, J. Power Sources 130 (2004) 111.
[7] D. Weng, J.S. Wainright, U. Landau, R.F. Savinell, J. Electrochem. Soc. 143 (1996) 1260.
[8] P. Musto, F.E. Karasz, W.J. MacKnight, Polymer 34 (1993) 2934.
[9] H.A. Pohl, R.P. Chartoff, J. Polym. Sci., Part A 2 (1964) 2787.
[10] S.M. Aharoni, A.J. Signorelli, J. Appl. Polym. Sci. 23 (1979) 2653.
[11] R. Bouchet, S. Miller, M. Duclot, J.L. Souquet, Solid State Ionics 145 (2001) 69.
[12] A. Schechter, R.F. Savinell, Solid State Ionics 147 (2002) 181.
[13] H. Pu, W.H. Meyer, G. Wegner, J. Polym. Sci., Part B 40 (2002) 663.
[14] R. He, Q. Li, G. Xiao, N.J. Bjerrum, J. Membr. Sci. 226 (2003) 169.
[15] Y.-L. Ma, J.S. Wainright, M.H. Litt, R.F. Savinell, J. Electrochem. Soc. 151 (2004) A8.
[16] J.A. Asensio, S. Borrós, P. Gómez-Romero, J. Electrochem. Soc. 151 (2004) A304.
[17] R.A. Munson, M.E. Lazarus, J. Phys. Chem. 71 (1967) 3245.
[18] T. Dippel, K.D. Kreuer, J.C. Lassègues, D. Rodriguez, Solid State Ionics 61 (1993) 41.

[19] M.F.H. Schuster, W.H. Meyer, M. Schuster, K.D. Kreuer, Chem. Mater. 16 (2004) 329.
[20] J.S. Wainright, J.-T. Wang, D. Weng, R.F. Savinell, M. Litt, J. Electrochem. Soc. 142 (1995) L121.
[21] Q. Li, R. He, R.W. Berg, H.A. Hjuler, N.J. Bjerrum, Solid State Ionics 168 (2004) 177.
[22] F. Barbir, J. Braun, J. Neutzler, J. New Mater. Electrochem. Syst. 2 (1999) 197.
[23] Q. Li, H.A. Hjuler, N.J. Bjerrum, J. Appl. Electrochem. 31 (2001) 773.
[24] K. Kinoshita, J. Electrochem. Soc. 137 (1990) 845.
[25] J.F. Shackelford, W. Alexander (Eds.), CRC Materials Science and Engineering Handbook, 3rd ed., CRC Press LLC, Boca Raton, 2001, p. 56 [online].
[26] J.F. Shackelford, W. Alexander (Eds.), CRC Materials Science and Engineering Handbook, 3rd ed., CRC Press LLC, Boca Raton, 2001, p. 58 [online].
[27] O.R. Hughes, P.N. Chen, W.M. Cooper, L.P. Disano, E. Alvarez, T.E. Andres, J. Appl. Polym. Sci. 53 (1994) 485.
[28] D. Bevers, M. Wöhr, K. Yasuda, K. Oguro, J. Appl. Electrochem. 27 (1997) 1254.
[29] J.S. Wainright, J.-T. Wang, R.F. Savinell, M. Litt, H. Moaddel, C. Rogers, in: S. Srinivasan, D.D. Macdonald, A.C. Khandkar (Eds.), Proceedings of the Electrochemical Society on Electrode Materials and Processes for Energy Storage and Conversion, vol. 94-23, 1994, pp. 255–264.
[30] T. Sakai, H. Takenaka, N. Wakabayashi, Y. Kawami, E. Torikai, J. Electrochem. Soc. 132 (1985) 1328.
[31] M. Thomassen, B. Børresen, G. Hagen, R. Tunold, Electrochim. Acta 50 (2004) 1157.
[32] A. Damjanovic, J.O'M. Bockris, Electrochim. Acta 11 (1966) 376.
[33] M.R. Tarasevich, A. Sadkowksi, E. Yeager, Comprehensive treatise of electrochemistry, in: B.E. Conway, J.O'M. Bockris, E. Yeager, S.U.M. Khan, R.E. White (Eds.), Kinetics and Mechanisms of Electrode Processes, vol. 7, Plenum Press, New York, 1983, pp. 301–398.
[34] D.A. Landsman, F.J. Luczak, in: W. Vielstich, H.A. Gasteiger, A. Lamm (Eds.), Handbook of Fuel Cells: Fundamentals, Technology and Applications, vol. 4: Fuel Cell Technology and Applications, John Wiley and Sons, Chichester, 2003, pp. 811–831.
[35] J.-T. Wang, R.F. Savinell, J. Wainright, M. Litt, H. Yu, Electrochim. Acta 41 (1996) 193.
[36] J.-T. Wang, J.S. Wainright, R.F. Savinell, M. Litt, J. Appl. Electrochem. 26 (1996) 751.
[37] Q. Li, H.A. Hjuler, C. Hasiotis, J.K. Kallitsis, C.G. Kontoyannis, N.J. Bjerrum, Electrochem. Solid-State Lett. 5 (2002) A125.
[38] O. Savadogo, B. Xing, J. New Mater. Electrochem. Syst. 3 (2000) 343.
[39] P. Staiti, F. Lufrano, A.S. Aricò, E. Passalacqua, V. Antonucci, J. Membr. Sci. 188 (2001) 71.